Analysis of the Contactless Power Transfer System Using Modeling and Analysis of the Contactless Transformer

Myunghyo Ryu†, Jonghyun Kim*, Juwon Baek* and Honnyong Cha**

Abstract - In this paper, the electrical characteristics of the contactless transformer is presented using the conventional coupled inductor theory. Compared with the conventional transformer, the contactless transformer has a large airgap, long primary wire and multi-secondary wire. As such, the contactless transformer has a large leakage inductance, small magnetizing inductance and poor coupling coefficient. Therefore, large magnetizing currents flow through the entire primary system due to small magnetizing inductance, resulting in low overall system efficiency.
In high power applications, the contactless transformer is so bulky and heavy that it needs to be split by some light and small transformers. So, the contactless transformer needs several small transformer modules that are connected in series or parallel to transfer the primary power to the secondary one.
This paper shows the analysis and measurement results of each contactless transformer module and comparison results between the series- and parallel-connection of the contactless transformer. The results are verified on the simulation based on the theoretical analysis and the 30kW experimental prototype.

Keywords: Contactless Transformer, Contactless Power Transfer System, Coupled Inductor Theory

1. Introduction

Nowadays, the Contactless Power Transfer System (CPTS) is widely used in many industrial applications such as automated guided vehicles and medical applications. Conventional ones drag long power cables directly to supply electrical power and produce many particles because of mechanical friction between power cables and the surfaces of nearby instruments, whereas CPTS delivers electrical power to load with the help of the contactless transformer that has no mechanical contact. In this method, the CPTS doesn't produce particles, thereby making it adaptable to the industrial applications where clean circumstances are needed such as in the case of semi-conductors, LCDs, and PDP manufacturing factories.

Fig. 1 shows the structure of the contactless transformer, which is composed of long primary wire and track over many meters, several transformer cores with a large airgap, and secondary winding wound around the transformer core. Since these kinds of transformers have low coupling coefficient (k) (normally lower than 0.5) because of the large airgap, it's very difficult to transfer primary energy to the secondary side. Also, since primary leakage inductance of the contactless transformer is larger than the magnetizing inductance, significant magnetizing currents flow through the magnetizing inductance. To solve these problems, a high frequency resonant converter (series resonant converter or series-parallel resonant converter) has been widely used for the CPTS [1~3].

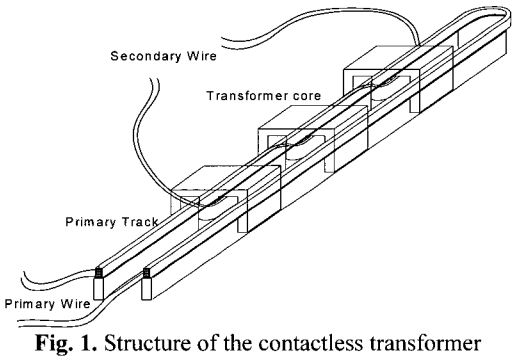

Fig. 1. Structure of the contactless transformer

In this paper, the electrical characteristics of the contactless transformer are presented using the conventional coupled inductor theory. The contactless transformer is constructed by adding many I-cores to make E-shape modules so that it can be fit for the primary track. To raise the power rating, contactless transformers have become so bulky and heavy that they are very difficult to handle and maintain. To solve those problems, contactless transformers need to be split with several small core modules to alleviate their weight and size by connecting these modules in series or parallel. By doing so, there are

† Corresponding Author: Industry Application Research Division, Korea Eletrotechnology Research Institute, Korea. (mhryu@keri.re.kr)
* Industry Application Research Division, Korea Eletrotechnology Research Institute, Korea. ({kimjh, jwbaek}@keri.re.kr)
** Electrical and computer Engineering, Michigan State University, USA. (chn92@hanmail.net)
Received: September 2, 2005 ; Accepted: June 14, 2006

some problems in modeling and analyzing contactless transformer parameters used for designing CPTS. Fig. 2 shows an E-shape contactless transformer module.

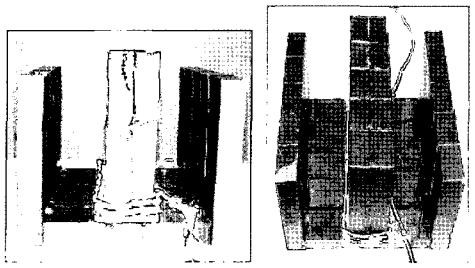

Fig. 2. E-shape contactless transformer module

This paper presents the analytical and numerical method to predict the parameters of the contactless transformer and can present design guidelines for designing the CPTS. Furthermore, the comparison between series connection and parallel connection of the contactless transformer is presented. The results are verified on the simulation based on the theoretical analysis and the 30kW experimental prototype.

2. Analysis of Contactless Power Transfer System

2.1 Series Resonant Converter

In general, the contactless transformer has a considerable airgap between the primary and secondary side and long primary wire that does not contact directly with the transformer core. Therefore, transformer leakage inductance is by far larger than magnetizing inductance. This results in poor coupling coefficient (k) and the overall system efficiency is reduced. In order to minimize the detrimental effects of large leakage inductance, small magnetizing inductance and poor coupling coefficient of contactless transformer, a full-bridge series resonant converter topology is selected for CPTS.

Fig. 3 shows a contactless power transfer system that adopts a full-bridge series resonant converter, where the magnetically coupled coil is replaced by a conventional transformer model containing leakage inductance (L_{lk}), magnetizing inductance (L_m) and ideal transformer with its turn ratio, "a".

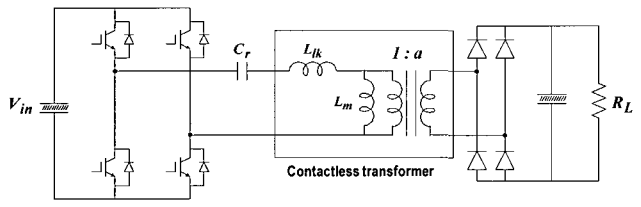

Fig. 3. Simplified circuit diagram of CPTS

2.2 Modeling and Analysis of Contactless Transformer

In this paper, the electrical characteristics of the contactless transformer are presented using conventional coupled inductor theory with self inductance (L_1, L_2) and mutual inductance (M). Fig. 4 indicates a basic model and T-equivalent model of the coupled inductor theory. We cannot ignore leakage inductance of the contactless transformer because of low coupling factor and small magnetizing inductance of the contactless transformer compared with that of conventional ones. Fig. 5 shows how to measure series inductance (L_{ser}) and parallel inductance (L_{par}) of the transformer.

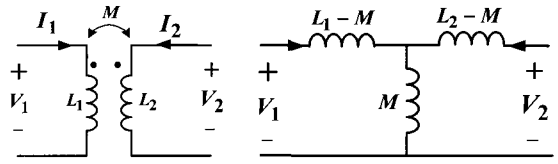

(a) Basic model (b) T-equivalent model

Fig. 4. Coupled inductor theory

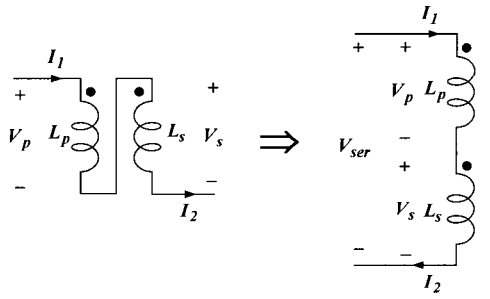

(a) Series inductance (L_{ser})

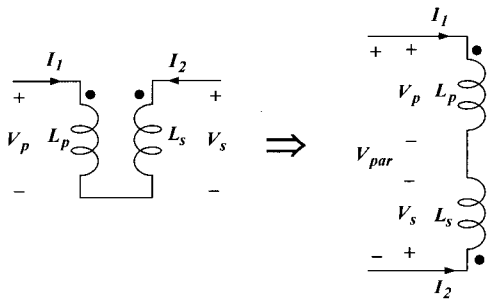

(b) Parallel inductance (L_{par})

Fig. 5. Measurement of L_{ser}, L_{par}

We can measure self inductances, L_1 and L_2, as Eqs. (1) and (2) from Faraday's law, when both the primary side and secondary side remains open. To measure mutual inductance, M, we must measure L_{ser} and L_{par}, and M is determined as Eq. (3)

$$V_1 = L_1 \frac{dI_1}{dt} + M \frac{dI_2}{dt} \tag{1}$$

$$V_2 = M\frac{dI_1}{dt} + L_2\frac{dI_2}{dt} \quad (2)$$

$$M = \frac{L_{ser} - L_{par}}{4} \quad (3)$$

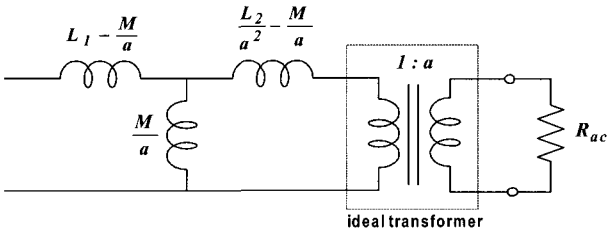

(a) Original model

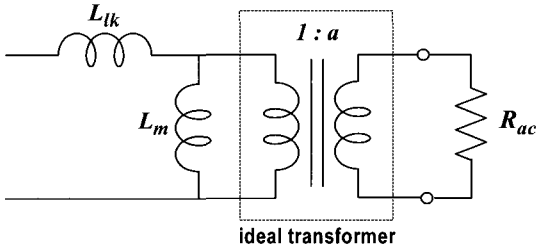

(b) Simplified model

Fig. 6. Equivalent model of the contactless transformer

Fig. 6 shows an equivalent model of the contactless transformer. In some cases, (L_2-M) can be a negative value because secondary self inductance (L_2) is less than mutual inductance (M). To make this value positive, mutual inductance is divided by arbitrary constant "a" [3]. In Fig. 6(a), its load resistance (R_L) is converted to AC resistance (R_{ac}) as defined in Eq. (4) [2], and arbitrary constant "a" (ideal turns ratio of the transformer) is shown as Eq. (5). Here, "a" may not be equal to the actual turn ratio of the transformer, "N_2/N_1", because coupling coefficient "k", which is shown as Eq. (6), is less than 1. If "k" becomes equal to 1, "a" is the same as "N_2/N_1" . In Fig. 6(b), L_{lk} and L_m are the leakage inductances and magnetizing inductance of magnetically coupled coils and are shown as Eqs. (7) and (8) respectively

$$R_{ac} = \frac{\pi^2}{8}R_L \quad (4)$$

$$a = \frac{L_2}{M} \quad (5)$$

$$k = \frac{M}{\sqrt{L_1 L_2}} \quad (6)$$

$$L_{lk} = L_1 - \frac{M}{a} = L_1(1-k^2) \quad (7)$$

$$L_m = \frac{M}{a} = L_1 k^2 \quad (8)$$

2.3 Series-Connection of Contactless Transformer

Fig. 7 shows a series-connected contactless transformer, of which primary and secondary sides are connected in series with each transformer module, diode rectifier, and load resistance. Each transformer is divided into two transformer models that are connected in series, and its load resistance is converted to AC resistance.

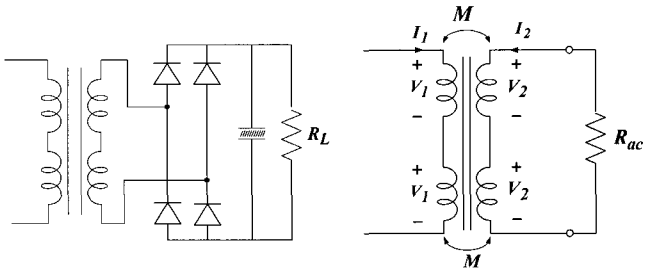

(a) (b)

Fig. 7. Series-connected contactless transformer

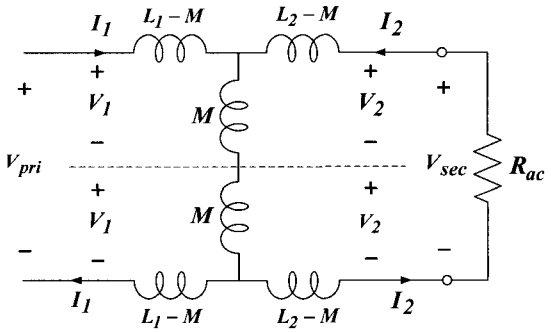

Fig. 8. T-equivalent model of series-connected contactless transformer

Fig. 8 shows the T-equivalent circuit model of Fig. 7, where V_{pri} and V_{sec} are the terminal voltages of the series-connected contactless transformer. From Faraday's law, Eqs. (9), (10), (11) and (12) represent terminal voltages V_1, V_2, V_{pri}, and V_{sec} related to the terminal currents I_1 and I_2 respectively.

$$V_1 = (L_1 - M)\frac{dI_1}{dt} + M\frac{d}{dt}(I_1 + I_2) \quad (9)$$

$$V_2 = (L_2 - M)\frac{dI_2}{dt} + M\frac{d}{dt}(I_1 + I_2) \quad (10)$$

$$V_{pri} = 2(L_1 - M)\frac{dI_1}{dt} + 2M\frac{d}{dt}(I_1 + I_2) \quad (11)$$

$$V_{sec} = 2(L_2 - M)\frac{dI_2}{dt} + 2M\frac{d}{dt}(I_1 + I_2) \quad (12)$$

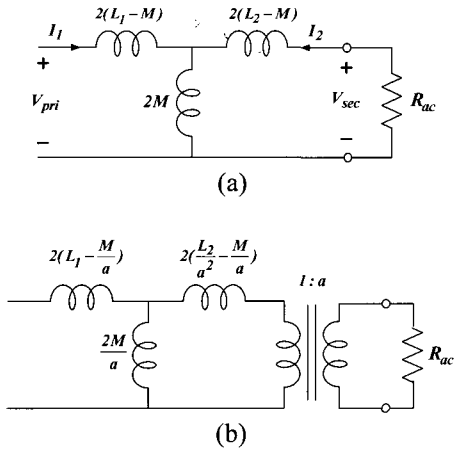

Fig. 9. Simplified circuit model of Fig. 8

Fig. 9 shows the simplified circuit model of the series-connected contactless transformer on the basis of Eqs. (11) and (12). Fig. 9(b) indicates the transformer model with insertion of the ideal transformer.

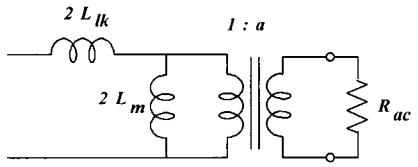

Fig. 10. Simplified model of the series-connected contactless transformer

If we let $2(\frac{L_2}{a^2}-\frac{M}{a})=0$, then $a=\frac{L_2}{M}$, where "a" is the ideal turn ratio of the transformer. Fig. 10 shows a simplified model of the series-connected contactless transformer.

From Fig. 10, leakage inductance($L_{lk}=L_1-\frac{M}{a}$) and magnetizing inductance($L_m=\frac{M}{a}$) are the measured values of each transformer module. Therefore, overall leakage inductance and magnetizing inductance of two series-connected contactless transformer modules become twice that of the single transformer module, leaving the ideal transformer turn ratio "a" unchanged. From the above mentioned result, if we connect the N number of transformer modules in series, then its total leakage and magnetizing inductance values become N times that of each transformer module. Whereas, the ideal transformer turn ratio remains unchanged.

2.4 Parallel-Connection of Contactless Transformer

Fig. 11 shows a parallel-connected contactless transformer in which the primary side is connected in series with each transformer module and the secondary side is connected in parallel with each transformer module and load resistance that is converted to AC load resistance using Eq. (4). Each AC load resistance is twice that of the single transformer module because voltage related to output is half of the total voltage.

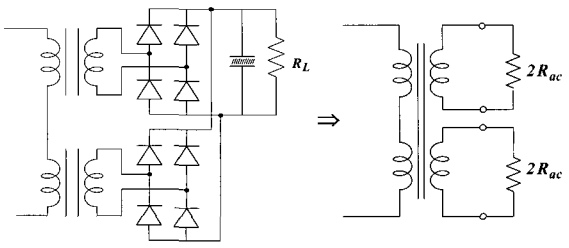

Fig. 11. Parallel-connected contactless transformer

Fig. 12 depicts an equivalent circuit model of Fig. 11 with its load resistance reflected to the primary side. In Fig. 12, L_{lk}, L_m, and "a" are the measured and analyzed values of each single transformer module just as in the case of series-connection. With simple numerical manipulation, Fig. 12 can be redrawn in Fig. 13 as a simplified contactless transformer model with its secondary side connected in parallel. From Fig. 13, the overall leakage inductance and magnetizing inductance of two parallel-connected contactless transformers becomes twice that of a single transformer module as in the case of series connection, but the ideal turn ratio of the transformer "a" becomes "a/2". If we extend this concept to the N secondary side parallel-connected contactless transformer, then total leakage inductance and magnetizing inductance values are N times those of each transformer module. Whereas the ideal turn ratio of the transformer becomes "a/N".

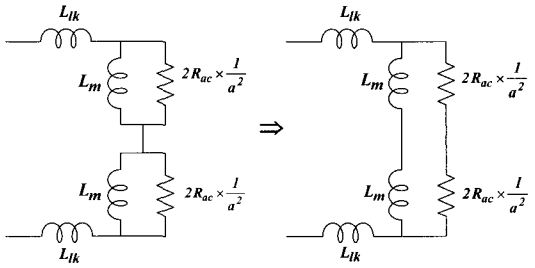

Fig. 12. Equivalent model of parallel-connected contactless transformer

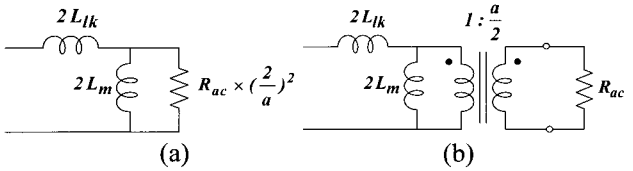

Fig. 13. Simplified model of parallel-connected contactless transformer

Table 1. Transformer parameters with N numbers of Module

	Series Connection	Parallel Connection
N number series- or Parallel-connected Transformer	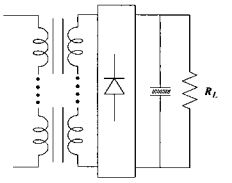	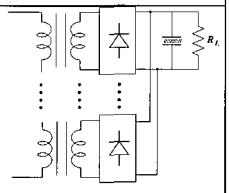
Simplified Equivalent Transformer Model	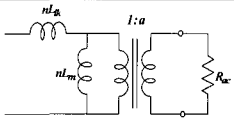	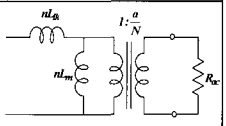
Leakage Inductance (L_{lk})	$L_{lk}'=NL_{lk}$	$L_{lk}'=NL_{lk}$
Magnetizing Inductance (L_m)	$L_m'=NL_m$	$L_m'=NL_m$
Ideal Turns Ratio (a)	a'=a	a'=a/N

* N is the module number of the transformer

Table 1 shows each contactless transformer parameter with N number series-connected transformer and N number parallel-connected transformer respectively.

2.4 Measurement Method of Transformer Parameters

Fig. 14 shows the measurement circuit of the transformer parameters. Since the contactless transformer has a long primary wire, primary winding inductance without transformer core is somewhat high, compared to conventional transformers. In Fig. 14, T_{out} represents the transformer model containing primary and secondary winding inductances (L_{wp}, L_{ws}), and T_{in} , which represents the transformer model except for the primary and secondary winding inductances. Here, L_{wp} and L_{ws} are winding inductances without magnetic core, T_{in} is conventional transformer model, and L_1 and L_2 represent primary and secondary self inductances containing L_{wp} and L_{ws} respectively.

If L_{ser} and L_{par} represent series inductance and parallel inductance of T_{in}, mutual inductance of T_{in}, M_{in} is described as;

$$M_{in} = \frac{L_{ser} - L_{par}}{4} \tag{13}$$

If L_{ser}' and L_{par}' represent series inductance and parallel inductance of T_{out}, mutual inductance of T_{out}, M_{out} is described as:

$$M_{out} = \frac{L_{ser}' - L_{par}'}{4} \tag{14}$$

Here,

$$L_{ser}' = L_{wp} + L_{ser} + L_{ws} \tag{15}$$

$$L_{par}' = L_{wp} + L_{par} + L_{ws} \tag{16}$$

Therefore,

$$M_{out} = M_{in} \tag{17}$$

If secondary winding inductance (L_{ws}) can be ignored, the ideal turn ratio of T_{out}, a_{out} is the same as the ideal turn ratio of T_{in}, a_{in} as Eq. (14)

$$a_{out} = \frac{L_2}{M_{out}} = \frac{L_s + L_{ws}}{M_{out}} \approx \frac{L_s}{M_{in}} = a_{in} \tag{18}$$

Therefore, we can measure the parameters of T_{in} and T_{out} respectively.

Fig. 15 illustrates the equivalent circuit of the contactless transformer containing primary and secondary winding inductances and the parameters of T_{in}. Here, L_{lk} and L_m are leakage inductance and magnetizing inductance of T_{in} and "a" is the ideal turn ratio of T_{in}.

Consequently, the total leakage inductance of T_{out} is the sum of L_{wp} and L_{lk}, ideal turn ratio of T_{out} is the same as that of T_{in}, and magnetizing inductance of T_{out} is the same as that of T_{in}.

We can measure the parameters of the contactless transformer, when primary and secondary winding inductance without magnetic core is measured and the parameters of T_{in} with short primary wire are measured.

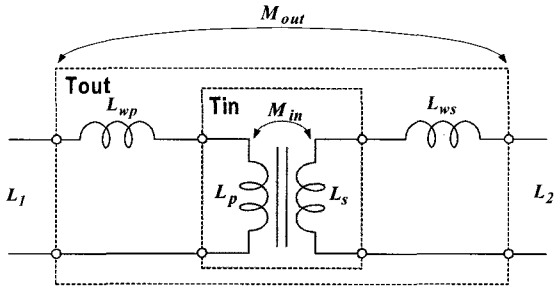

Fig. 14. Measurement circuit of the transformer parameters

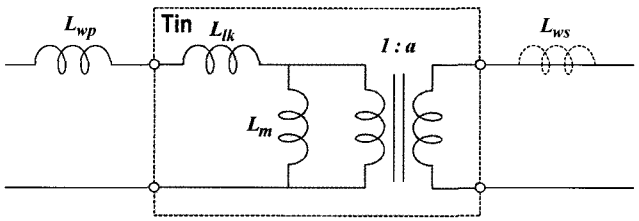

Fig. 15. Equivalent circuit for measurement of the transformer parameters

3. Measurement Results of Transformer Parameters

Table 2. Specifications of the contactless transformer

Winding number	Primary	2turns
	Secondary	3.5turns
Primary wire length		120m
Core size		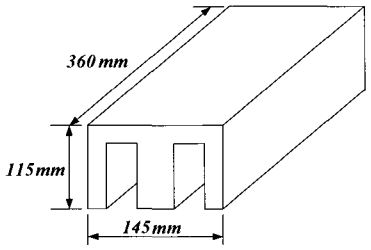
Primary winding inductance (L_{wp})		72uH
Secondary winding inductance (L_{ws})		2uH
Primary winding resistance		47.5mΩ

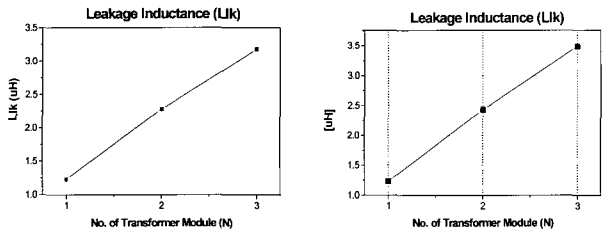

(a) Leakage inductance vs. No. of transformer modules

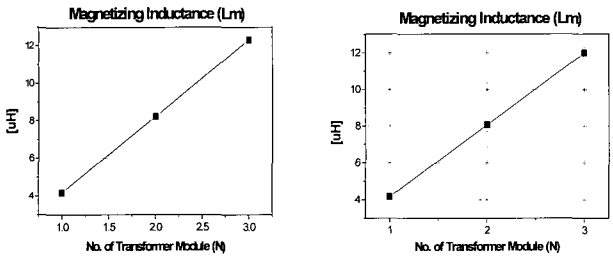

(b) Magnetizing inductance vs. No. of transformer modules

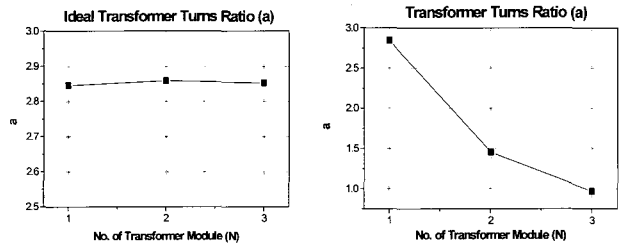

(c) Turn ratio vs. No. of transformer modules

Fig. 16. Comparison of measurement results between series- and parallel-connected contactless transformers

Table 2 shows the specifications of the contactless transformer used in the test. Each transformer module was manufactured with single I-type cores. Measured primary and secondary winding inductance and primary winding resistance are 72uH, 2uH, and 47.5mΩ, respectively.

Table 3. Measurement results of the series-connected contactless transformer

	1 module	2 module	3 module
Primary self inductance (L_p=L_1-L_{wp}, uH)	5.4	10.5	15.5
Secondary self inductance (L_s=L_2-L_{ws}, uH)	33.8	67.2	100.3
L_{ser}=L_{ser}'-L_{wp} (uH)	63.2	124.7	186.2
L_{par}=L_{par}'-L_{wp} (uH)	15.7	30.7	45.6
Mutual inductance (M, uH)	11.9	23.5	35.2
Leakage inductance (L_{lk}, uH)	1.2	2.3	3.2
Magnetizing inductance (L_m, uH)	4.2	8.22	12.3
Coupling Coefficient(k)	0.88	0.88	0.89
Ideal turn ratio(a)	2.85	2.86	2.85

Table 4. Measurement results of the parallel-connected contactless transformer

	1 module	2 module	3 module
Primary self inductance (L_p=L_1-L_{wp}, uH)	5.4	10.5	15.5
Secondary self inductance (L_s=L_2-L_{ws}, uH)	33.8	17.1	11.5
L_{ser}=L_{ser}'-L_{wp} (uH)	63.2	49.2	50.2
L_{par}=L_{par}'-L_{wp} (uH)	15.7	2.2	2.7
Mutual inductance (M, uH)	11.9	11.8	11.9
Leakage inductance (L_{lk}, uH)	1.2	2.4	3.2
Magnetizing inductance (L_m, uH)	4.2	8.1	12.3
Coupling Coefficient (k)	0.88	0.88	0.89
Ideal turn ratio (a)	2.85	1.46	0.97

Table 3, Table 4 and Fig. 16 show measurement results of the series- and parallel-connected contactless transformer. As shown in Fig. 16, measurement results are the same as the analysis results.

4. Simulation and Experimental Results of Contactless Power Transfer System

A 30kW experimental CPTS prototype was built and

tested to verify analysis and measurement results (Fig. 3). Table V shows the parameters used in the simulation and experiment. Parameters measured in Section III were used in the test, too.

Table 5. Parameters used in simulation and experiment

Winding number	Primary	2turns
	Secondary	3.5turns
Number of modules		3EA
Resonant capacitance (Cr)		1.32uF
Primary winding inductance (Lwp)		72uH
Leakage inductance of each module (Llk)		1.2uH
Total leakage inductance ((Lwp+3Llk)		75.6uH
Magnetizing inductance of each module (Lm)		4.2uH
Total magnetizing inductance (3Lm)		12.6uH
Ideal turn ratio (a)		2.85

Fig. 17 shows voltage gain and phase response of input impedance according to frequency and load change using the equivalent model of the series-connected contactless transformer and parameters of Table V.

Fig. 18 presents simulation and experimental results of the full-bridge output voltage and resonant current at 24kW output power. In the figure, the simulation result and experimental result are equivalent. This indicates that the parameters used in the test are suitable for the contactless power transfer system.

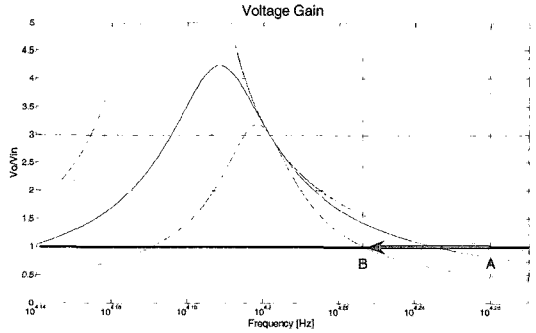

(a) Voltage gain vs. frequency

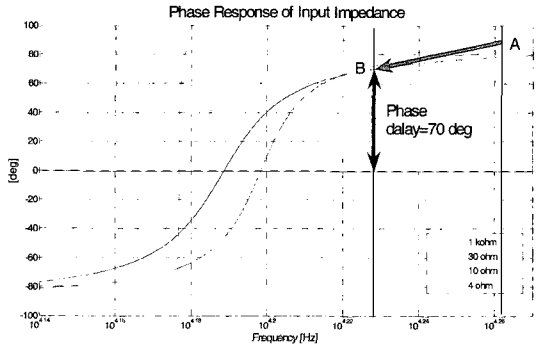

(b) Phase margin vs. frequency

Fig. 17. Frequency analysis results

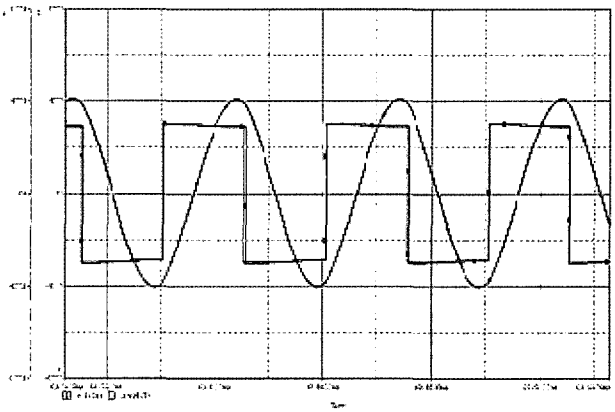

(a) Simulation result

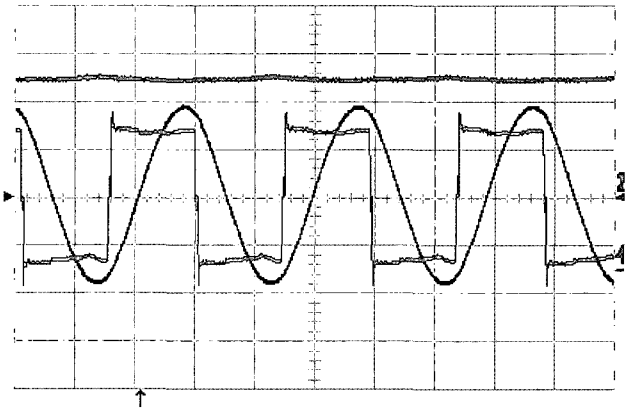

(b) Experimental result

Fig. 18. Simulation and experimental results (Vo=300V, Io=80A, Po=24kW) (voltage: 200V/div. Current: 200A/div.)

5. Conclusion

In this paper, the electrical characteristics of the contactless transformer are presented using the conventional coupled inductor theory. Through analysis and measurement, simplified models of the series- and parallel-connected contactless transformer were induced related to the single contactless transformer module. And, measurement methods of the transformer parameters were introduced and measurement results verified the analysis results.

A 30kW experimental CPTS prototype was built and tested to verify analysis and measurement results. The experimental results are the same as the analysis and measurement results.

References

[1] Byungcho Choi, Jaehyun Noh, Honnyong Cha, Taeyoung Ahn and Seungwon Choi, "Design and

Implementation of Low-profile Contactless Battery Charger Using Planar Printed Circuit Board Windings as Energy Transfer Device," IEEE Trans. Industrial Electronics, vol. 51, no. 1, pp. 7-10, Feb. 2004.

[2] G. B. Joung, and B. H. Cho, "An Energy Transmission System for an Artificial Heart Using Leakage Inductance Compensation of Transcutaneous Transformer", in IEEE Trans, PE, Vol. 13, 1998.

[3] A. Ghahary, and B. H. Cho, "Design of a Transcutaneous Energy Transmission System Using a Series Resonant Converter", in IEEE Power Electronics Specialists Conf. Rec., pp. 1-8, 1990.

[4] Robert L. Steigerwald, "A Comparison of Half-Bridge Resonant Converter Topologies," IEEE Trans. Power Electronics, vol. 3, pp. 174-182, Apr. 1988.

[5] Don A. G. Pedder, Andrew D. Brown, J. Andrew Skinner, "A Contactless Electrical Energy Transmission System", in IEEE Trans, industrial electronics, Vol. 46, No. 1, 1999.

[6] Yungtaek Jang and Mila M. Jovanovic, "A Contactless Electrical Energy Transmission System for Portable-Telephone Battery Charger", in IEEE Trans, industrial electronics, Vol. 50, No. 3, 2003.

Myunghyo Ryu

He received his B.S. and M.S. degrees in Electrical Engineering from Kyungpook National University, Taegu, Korea, in 1997 and 1999, respectively. Currently, he is a Researcher in the Power Electronics Group, Korea Electrotechnology Research Institute (KERI). His research interests are the DC/DC converter, resonant converter, and high voltage applications.

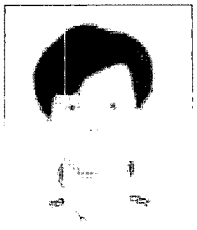

Jonghyun Kim

He was born on Apr. 18, 1968 and received his Ph.D. degree in Electronic and Electrical Engineering from Pohang University of Science and Technology. His main research interests are module type DC-DC converters and inverters for the LCD Back-light technique. He is currently a Senior Researcher in the Power Electronics Group, Korea Electrotechnology Research Institute (KERI).

Juwon Baek

He received his M.S. and Ph. D. degrees from Kyungpook National University, Taegu, Korea in 1993 and 2002, respectively.

Since 1993, he has been with the Power Electronics Research group at the Korea Electrotechnology Research Institute (KERI) as a Senior Researcher. Also, he worked at FEEC (Future Energy Challenge Center) of Virginia tech as a Visiting Scholar in 2004. His primary research areas include soft switching converters, power factor correction circuits, power quality, high voltage power supplies, and power converters for renewable energy.

He is a member of various organizations including IEEE, KIEE and KIPE.

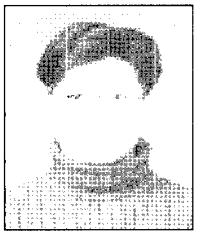

Honnyong Cha

He received his B.S. and M.S. degrees in Electrical Engineering in 1999 and 2001, respectively, from Kyungpook National University, Taegu, Korea. He is currently working toward a Ph.D. degree at Michigan State University. His research interests include modeling, analysis, and design of power converters.